Acta Crystallographica Section F
Structural Biology and Crystallization Communications
ISSN 1744-3091

Purification, crystallization and preliminary X-ray diffraction analysis of the lytic transglycosylase MltF from *Escherichia coli*

Pramod K. Madoori and Andy-Mark W. H. Thunnissen*

Department of Biophysical Chemistry, Groningen Biomolecular Sciences and Biotechnology Institute, University of Groningen, Nijenborgh 4, 9747 AG Groningen, The Netherlands

Correspondence e-mail: a.m.w.h.thunnissen@rug.nl

Received 6 December 2009
Accepted 21 March 2010

The lytic transglycosylase MltF from *Escherichia coli* is an outer-membrane-bound periplasmic protein with two domains: a C-terminal catalytic domain with a lysozyme-like fold and an N-terminal domain of unknown function that is homologous to the periplasmic substrate-binding proteins of ABC transporters. In order to investigate its structure and function, a soluble form of full-length MltF (sMltF) containing both domains and a soluble fragment containing only the N-terminal domain (sMltF-NTD) were purified and crystallized. Crystals of sMltF belonged to space group $P4_32_12$ or $P4_12_12$, with unit-cell parameters $a = b = 110.8$, $c = 163.5$ Å and one or two molecules per asymmetric unit. A complete data set was collected to 3.5 Å resolution. Crystals of sMltF-NTD belonged to space group $P3_121$, with unit-cell parameters $a = b = 82.4$, $c = 75.2$ Å and one molecule per asymmetric unit. For sMltF-NTD, a complete native data set was collected to 2.20 Å resolution. In addition, for phasing purposes, a three-wavelength MAD data set was collected to 2.5 Å resolution using a bromide-soaked sMltF-NTD crystal. Using phases derived from the Br-MAD data, it was possible to build a partial model of sMltF-NTD.

1. Introduction

The viability and shape of bacteria depend on the presence of an intact cell wall that surrounds their cytoplasmic membrane. The integral component of the bacterial cell wall is a heteropolymer known as peptidoglycan (PG) or murein. It is composed of glycan strands consisting of alternating β-1,4-linked *N*-acetylmuramic acid (MurNAc) and *N*-acetylglucosamine (GlcNAc) residues cross-linked by peptides that are connected to the lactyl groups of the MurNAc residues (Vollmer *et al.*, 2008). The mesh-like PG structure gives the cell wall its mechanical strength, allowing bacterial cells to withstand high internal osmotic pressures. Once synthesized, however, the PG polymer is not a static macromolecule but is subject to continuous remodelling and turnover (Park & Uehara, 2008). In particular, PG cleavage is required to create space for the insertion of new material and to recycle old material during cell growth, to incise the cell wall during cell division and to create local openings in the cell wall to allow the insertion of various cell envelope-spanning structures (Höltje, 1998; Koraimann, 2003; Scheurwater *et al.*, 2008). PG cleavage is carried out by bacterial glycolytic and peptidolytic enzymes that are referred to as autolysins. Some of these bacterial enzymes are crucial for bacterial pathogenicity and have been shown to modulate muropeptide release and/or host innate immune responses (Lee *et al.*, 2009).

Lytic transglycosylases (LTs) form one set of autolysins that target the β-1,4-linkages between the MurNAc and GlcNAc residues of PG (Höltje, 1996; Scheurwater *et al.*, 2008). They act like lysozymes and other β-1,4-glycosyl hydrolases, but differ with respect to the reaction products. Strictly speaking, LTs are glycosyl transferases, not hydrolases, and combine the cleavage of an inter-residue β-1,4-glycosidic bond with the formation of an intra-residue 1,6-glycosidic bond, thereby producing 1,6-anhydromuropeptides (Fig. 1). LTs are ubiquitous among all eubacteria that produce PG, but the complement of enzymes produced by *Escherichia coli* has been the most extensively examined. *E. coli* is known to produce six outer-membrane-bound

lytic transglycosylases (MltA, MltB, MltC, MltD, MltE and MltF) and one soluble lytic transglycosylase (Slt70) (for reviews, see Höltje, 1996; Scheurwater *et al.*, 2008). Most appear to act as exo-enzymes, releasing anhydromuropeptides from the ends of glycan strands; the exception is MltE, which has been shown to be endo-acting (Kraft *et al.*, 1998). Collectively, these enzymes form the archetypes of three of the four families of LTs identified by Blackburn & Clarke (2001). Crystal structures, complemented by sugar-binding and muropeptide-binding studies, have been reported for Slt70 (Thunnissen *et al.*, 1994; van Asselt, Thunnissen *et al.*, 1999), MltA (van Straaten *et al.*, 2005, 2007) and Slt35 (a soluble proteolytic fragment of MltB; van Asselt, Dijkstra *et al.*, 1999; van Asselt *et al.*, 2000), representing LT families I, II and III, respectively. These crystallographic studies allowed a thorough understanding of the structures and catalytic mechanism of LTs and revealed that most of these enzymes, with the exception of MltA, share a catalytic domain that resembles the fold of goose-type lysozyme (Thunnissen *et al.*, 1995). However, the specific roles of the different *E. coli* LTs in PG metabolism remain unclear (Heidrich *et al.*, 2002), which is emphasized by the fact that most LTs contain additional noncatalytic domains for which the function is often unknown.

MltF from *E. coli* is a recently characterized member of LT family I, which based on sequence analysis and functional assays contains a typical lysozyme-like C-terminal domain (hereafter named the LT domain) that is responsible for its LT activity (Scheurwater & Clarke, 2008). As a unique feature, however, it contains an N-terminal domain homologous to the periplasmic substrate-binding proteins of ABC transporters, in particular to those specific for histidine, lysine–arginine–ornithine (LAO) and glutamine (Tam & Saier, 1993). The function of this N-terminal domain (MltF-NTD) is unknown. No peptidoglycan-binding activity could be measured for MltF-NTD, nor have any ligands been identified that may form substrates of this domain (Scheurwater & Clarke, 2008). The N-terminal domain has been shown to modulate the lytic activity of the LT domain to permit the continued lysis of insoluble peptidoglycan at a constant rate (Scheurwater & Clarke, 2008), but how this modulation happens is currently not understood.

To obtain insights into the role of the N-terminal domain of MltF and how it may affect the catalytic function of the LT domain, we studied MltF using X-ray crystallographic and biochemical methods. In this paper, we describe the purification, crystallization and preliminary X-ray analysis of two soluble C-terminally His_6-tagged forms of MltF, one containing both domains (sMltF) and one containing only the N-terminal domain (sMltF-NTD).

2. Materials and methods

2.1. Expression and purification

Soluble MltF (sMltF; 511 residues), lacking the predicted signal sequence and transmembrane helix (residues 2–22 in MltF) but with an extra C-terminal His_6 tag (sequence KLAAALEHHHHHH), was expressed using the previously published expression vector pACES-8 (Scheurwater & Clarke, 2008). Expression was carried out in *E. coli* strain Rosetta 2 (DE3) pLysS (Novagen). A 2 l LB culture supplemented with chloramphenicol (34 µg ml^{-1}) and kanamycin (50 µg ml^{-1}) was incubated at 310 K until the $OD_{600\,nm}$ reached ∼0.6. The cells were then induced by the addition of 1 m*M* isopropyl *β*-D-1-thiogalactopyranoside (IPTG) and incubated for an additional 3 h at 310 K. For the preparation of soluble fractions, cultured cells were harvested by centrifugation at 8000 rev min^{-1} for 20 min at 277 K and the resulting bacterial pellet was resuspended in 50 ml ice-cold lysis buffer containing 20 m*M* Tris–HCl pH 8.0, 300 m*M* NaCl, 2 m*M* imidazole, 0.2% NP-40, 10 m*M* *β*-mercaptoethanol and appropriate amounts of DNase, RNase and protease inhibitors (Roche Applied Science). Cells were lysed using a French press and the soluble proteins were collected by centrifugation at 10 000 rev min^{-1} for 20 min at 277 K. The supernatant was applied onto a 0.5 ml Ni–NTA (Qiagen) column pre-equilibrated with 20 m*M* Tris–HCl pH 8.0, 300 m*M* NaCl, 10 m*M* imidazole and 1 m*M* *β*-mercaptoethanol (buffer *A*). The column was washed with 3–4 column volumes of buffer *A* to remove unbound proteins and sMltF was eluted with 200 m*M* imidazole in buffer *A*. Elution fractions containing sMltF were pooled, diluted sixfold in buffer *B* [20 m*M* Tris–HCl pH 8, 1 m*M* EDTA and 1 m*M* dithiothreitol (DTT)] and subsequently loaded onto a MonoQ column (GE Healthcare) which was equilibrated with buffer *B*. Elution was carried out with a gradient of increasing NaCl concentration from 50 to 500 m*M*. The peak fractions containing sMltF were pooled and concentrated to 12 mg ml^{-1} in 20 m*M* Tris–HCl pH 8.0, 50 m*M* NaCl, 1 m*M* EDTA and 1 m*M* DTT using an Amicon ultrafiltration centrifugal device (Millipore).

Expression and purification of the N-terminal domain of sMltF (sMltF-NTD; residues 23–250 of MltF with an additional C-terminal His_6 tag) followed a similar procedure as used for the full-length protein. Expression was carried out with the vector pACES-13 (Scheurwater & Clarke, 2008) in C43 (DE3) *E. coli* cells using LB medium supplemented with kanamycin. A three-step purification protocol using Ni–NTA, Mono Q and gel-filtration chromatography was applied to obtain pure protein. The Ni–NTA and MonoQ purification steps were performed as for sMltF. Gel filtration was carried out on a Superdex 200 column (GE Healthcare) pre-equilibrated with column buffer containing 50 m*M* Tris–HCl pH 8, 50 m*M* NaCl and 1 m*M* DTT. The peak fractions containing sMltF-NTD were pooled and concentrated to 6 mg ml^{-1} in gel-filtration column buffer. Protein concentrations were estimated from the absorbance at 280 nm (A_{280}) using theoretical molar extinction coefficients of 84 230 and 38 390 M^{-1} cm^{-1} for sMltF and sMltF-NTD, respectively.

All purification steps were performed at 280 K and the results of each step were monitored by SDS–PAGE. The final protein samples were highly pure (>98%) and monodisperse as judged from silver-stained SDS–PAGE gels and dynamic light-scattering experiments (DynaPro, Wyatt Technology), respectively. After concentration, the protein samples were quickly frozen in liquid nitrogen or used immediately for crystallization screening.

2.2. Crystallization

Screening for initial crystallization conditions was performed using the sitting-drop vapour-diffusion method with the aid of an Oryx-6 crystallization robot (Douglas Instruments) at room temperature (298 K) using the commercial JCSG+ and PACT crystallization screens (Molecular Dimensions Ltd). Lead conditions for crystallization were further optimized by changing the salt concentration, precipitant concentration, temperature and buffering agents. Crystal-

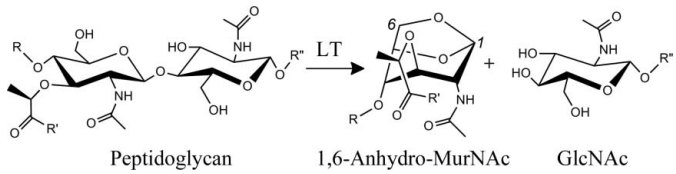

Figure 1
LTs catalyze the cleavage of the *β*-1,4-glycosidic bonds between MurNAc and GlcNAc residues in PG, with the concomitant formation of a 1,6-anhydro-MurNAc residue.

Table 1
Summary of the X-ray data for full-length sMltF.

Values in parentheses are for the highest resolution shell.

Beamline	ID23-2
Detector	MAR Mosaic 225
Wavelength (Å)	0.873
Crystal-to-detector distance (mm)	306.1
Oscillation angle (°)	0.8
No. of recorded images	96
Space group	$P4_32_12$ or $P4_12_12$
Unit-cell parameters (Å)	$a = b = 110.8$, $c = 163.5$
Solvent content (%)	44 or 72
Resolution range (Å)	49.5–3.5
Total No. of observations	55062 (7923)
No. of unique reflections	12980 (1864)
Multiplicity	4.2 (4.3)
Completeness (%)	97.2 (98.0)
$R_{\rm merge}$† (%)	12.3 (21.5)
Mean $I/\sigma(I)$	8.6 (5.9)

† $R_{\rm merge} = \sum_{hkl}\sum_i |I_i(hkl) - \langle I(hkl)\rangle| / \sum_{hkl}\sum_i I_i(hkl)$, where $I_i(hkl)$ is the ith observation of reflection hkl and $\langle I(hkl)\rangle$ is the the weighted average intensity for all observations i of reflection hkl.

optimization experiments were performed manually using the hanging-drop vapour-diffusion method by mixing and equilibrating equal volumes (1 µl) of protein and reservoir solution against 500 µl reservoir solution in a 24-well plate. Tetragonal crystals of sMltF measuring 80 × 40 × 20 µm were grown from 0.1 *M* ammonium acetate, 0.1 *M* bis-tris pH 5.5, 15% PEG 10 000 and trigonal crystals of sMltF-NTD with dimensions of 200 × 60 × 60 µm were grown from 0.15 *M* lithium sulfate, 0.1 *M* sodium citrate pH 5.5, 20% PEG 3350.

2.3. X-ray data collection and processing

X-ray diffraction data were collected at the ESRF, Grenoble using cryocooled crystals. Full-length sMltF crystals were cryoprotected by increasing the PEG 10 000 concentration to 30%. Cryoprotection of the sMltF-NTD crystals required the addition of 15% glycerol to the crystallization solution. Data were integrated using *XDS* (Kabsch, 1993) and scaled and merged into unique data sets with the programs *SCALA* and *TRUNCATE* from the *CCP*4 suite (Collaborative Computational Project, Number 4, 1994). The sMltF crystals suffered from extensive radiation damage, resulting in a somewhat poor overall quality of the data set and a useful resolution of only 3.5 Å, even though diffraction extended to about 2.5 Å at the beginning of the data-collection experiment. The sMltF-NTD crystals, on the other hand, were very stable in the X-ray beam and diffracted to 2.2 Å resolution. In addition to a native data set, a three-wavelength Br-MAD data set was collected from a single MltF-NTD crystal that was soaked for 15–20 s in a solution containing 20% glycerol and 0.6 *M* NaBr just prior to freezing, following published protocols (Dauter *et al.*, 2000). Tables 1 and 2 list the relevant data-collection statistics.

3. Results and discussion

Both full-length sMltF and sMltF-NTD were successfully purified and crystallized. X-ray data were collected from cryocooled crystals using the MX beamlines at the ESRF, Grenoble. Crystals of sMltF diffracted to a maximum resolution of 2.5 Å (Fig. 2*a*), but owing to radiation damage the finally obtained unique data set was only complete to 3.5 Å resolution (Table 1). The space group was identified as $P4_32_12$ or $P4_12_12$, with unit-cell parameters $a = b = 110.8$, $c = 163.5$ Å. Computation of the Matthews coefficient indicated that the asymmetric unit contains either one protein molecule (Matthews coefficient of 4.4 Å^3 Da^{-1}) or two protein molecules (Matthews coefficient of 2.2 Å^3 Da^{-1}), with a solvent content of 72% or 44%, respectively. A Patterson self-rotation map did not reveal the presence of any rotational noncrystallographic symmetry (NCS), nor was any translational NCS detected in a native Patterson map, indicating that the asymmetric unit probably contains a single protein molecule. In solution, sMltF behaves as a monomer based on gel-filtration chromatography and static light-scattering analysis (not shown). It cannot be excluded, however, that an NCS peak that is present in the self-rotation map is obscured by a crystallographic symmetry-axis peak.

Table 2
Summary of the X-ray data for sMltF-NTD.

Values in parentheses are for the highest resolution shell.

		Br-MAD		
	Native	Peak	Inflection	Remote
Beamline	ID29	BM16		
Detector	ADSC Q315r	ADSC Q210r		
Wavelength (Å)	0.9300	0.9198	0.9206	0.8569
Crystal-to-detector distance (mm)	360.2	288.1		
Oscillation angle (°)	1.0	1.0		
No. of recorded images	120	130		
Space group	$P3_121$	$P3_121$		
Unit-cell parameters (Å)	$a = b = 82.4$, $c = 75.2$	$a = b = 82.6$, $c = 75.2$		
Solvent content (%)	51	51		
Resolution range (Å)	71.4–2.2	41.4–2.6	41.3–2.7	41.4–2.8
Unique reflections	15240	9004	8503	7526
Multiplicity	7.0	8.0	8.0	8.0
Completeness (%)	100 (98.3)	100 (98.5)	100 (99)	100 (99)
$R_{\rm merge}$† (%)	5.5 (47.0)	8.0 (48.1)	10.6 (64.0)	9.5 (53.0)
Mean $I/\sigma(I)$	19.1 (4.2)	20.5 (4.6)	17.0 (3.5)	18.2 (4.2)

† $R_{\rm merge} = \sum_{hkl}\sum_i |I_i(hkl) - \langle I(hkl)\rangle| / \sum_{hkl}\sum_i I_i(hkl)$, where $I_i(hkl)$ is the ith observation of reflection hkl and $\langle I(hkl)\rangle$ is the the weighted average intensity for all observations i of reflection hkl.

Crystals of sMltF-NTD allowed the collection of a complete data set to 2.2 Å resolution (Table 2; Fig. 2*b*). Based on these data, the space group of the sMltF-NTD crystals was initially determined to be $P3_121$ or $P3_221$, with unit-cell parameters $a = b = 82.4$, $c = 75.2$ Å and a single molecule per asymmetric unit (with a solvent content of 51%). Molecular replacement was tried as a method to obtain initial phases for the sMltF and sMltF-NTD diffraction data using search models based on the LT domain of Slt70 and on various structures of periplasmic substrate-binding proteins, but without success. However, in an alternative approach to obtain phases a three-wavelength MAD data set was collected to 2.7 Å resolution from a single bromide-soaked crystal of sMltF-NTD (Table 2). Phase calculation and refinement were performed in both space groups ($P3_121$ or $P3_221$) using the program *SHARP*/*autoSHARP* (Vonrhein *et al.*, 2007) followed by density modification with *SOLOMON* (Abrahams & Leslie, 1996). Three different bromide sites were identified in the asymmetric unit and the best set of phases was calculated in space group $P3_121$. The overall figure of merit (FOM) was 0.43 and 0.90 before and after solvent flipping, respectively, for reflections in the resolution range 71.7–3.0 Å. The resulting experimental electron-density map showed clear solvent–protein boundaries and features of secondary-structural elements were clearly visible in the protein-associated densities. Using automated model building (Terwilliger, 2003), it was possible to fit a partial model of nearly 137 amino acids (52% of the complete protein) into the electron-density map. Further model building and refinement of the sMltF-NTD structure is in progress and will be reported elsewhere. In addition, the crystallization conditions for full-length sMltF are currently being optimized in order to obtain better quality crystals.

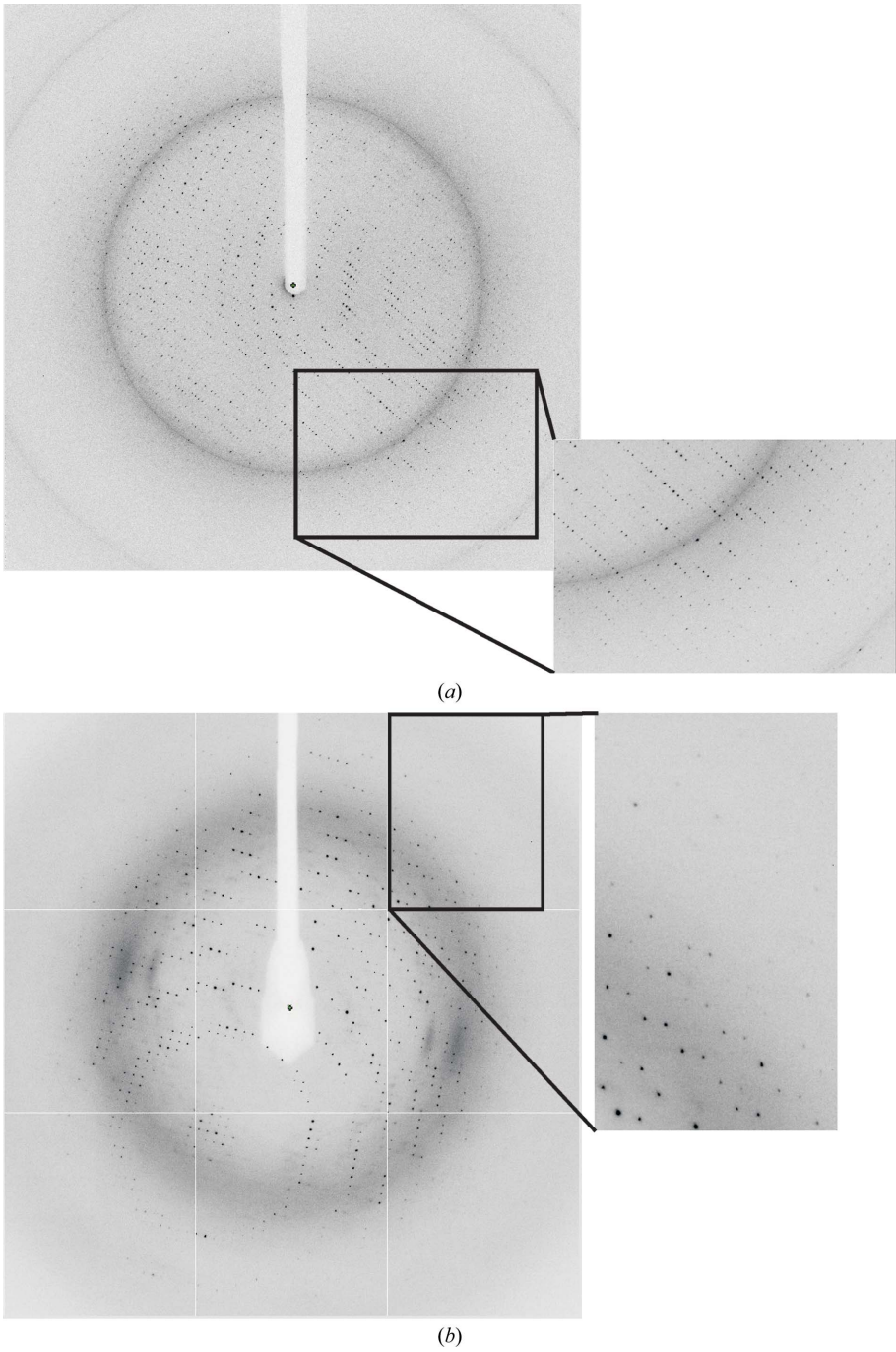

Figure 2
Diffraction images of sMltF crystals: (*a*) full-length protein, (*b*) sMltF-NTD. The edge of the detector corresponds to 1.8 and 1.7 Å in (*a*) and (*b*), respectively. The insets display the quality and maximum resolution of the diffraction.

The authors thank Edie M. Scheurwater and Anthony J. Clarke (University of Guelph, Canada) for providing the expression vectors for producing the soluble MltF proteins. This research was supported in part by an Ubbo Emmius Bursary, University of Groningen awarded to PKM.

References

Abrahams, J. P. & Leslie, A. G. W. (1996). *Acta Cryst.* D**52**, 30–42.
Asselt, E. J. van, Dijkstra, A. J., Kalk, K. H., Takacs, B., Keck, W. & Dijkstra, B. W. (1999). *Structure*, **7**, 1167–1180.
Asselt, E. J. van, Kalk, K. H. & Dijkstra, B. W. (2000). *Biochemistry*, **39**, 1924–1934.
Asselt, E. J. van, Thunnissen, A.-M. W. H. & Dijkstra, B. W. (1999). *J. Mol. Biol.* **291**, 877–898.
Blackburn, N. T. & Clarke, A. J. (2001). *J. Mol. Evol.* **52**, 78–84.
Collaborative Computational Project, Number 4 (1994). *Acta Cryst.* D**50**, 760–763.
Dauter, Z., Dauter, M. & Rajashankar, K. R. (2000). *Acta Cryst.* D**56**, 232–237.
Heidrich, C., Ursinus, A., Berger, J., Schwarz, H. & Höltje, J.-V. (2002). *J. Bacteriol.* **184**, 6093–6099.
Höltje, J. V. (1998). *Microbiol. Mol. Biol. Rev.* **62**, 181–203.
Höltje, J. V. (1996). *EXS*, **75**, 425–429.
Kabsch, W. (1993). *J. Appl. Cryst.* **26**, 795–800.

Koraimann, G. (2003). *Cell. Mol. Life Sci.* **60**, 2371–2388.
Kraft, A. R., Templin, M. F. & Höltje, J. V. (1998). *J. Bacteriol.* **180**, 3441–3447.
Lee, M., Zhang, W., Hesek, D., Noll, B. C., Boggess, B. & Mobashery, S. (2009). *J. Am. Chem. Soc.* **131**, 8742–8743.
Park, J. T. & Uehara, T. (2008). *Microbiol. Mol. Biol. Rev.* **72**, 211–227.
Scheurwater, E. & Clarke, A. J. (2008). *J. Biol. Chem.* **283**, 8363–8373.
Scheurwater, E., Reid, C. W. & Clarke, A. J. (2008). *Int. J. Biochem. Cell Biol.* **40**, 586–591.
Straaten, K. E. van, Barends, T. R., Dijkstra, B. W. & Thunnissen, A.-M. W. H. (2007). *J. Biol. Chem.* **282**, 21197–21205.
Straaten, K. E. van, Dijkstra, B. W., Vollmer, W. & Thunnissen, A.-M. W. H. (2005). *J. Mol. Biol.* **352**, 1068–1080.
Tam, R. & Saier, M. H. Jr (1993). *Microbiol. Rev.* **57**, 320–346.
Terwilliger, T. C. (2003). *Acta Cryst.* D**59**, 1174–1182.
Thunnissen, A.-M. W. H., Dijkstra, A. J., Kalk, K. H., Rozeboom, H. J., Engel, H., Keck, W. & Dijkstra, B. W. (1994). *Nature (London)*, **367**, 750–753.
Thunnissen, A.-M. W. H., Isaacs, N. W. & Dijkstra, B. W. (1995). *Proteins*, **22**, 245–258.
Vollmer, W., Blanot, D. & de Pedro, M. A. (2008). *FEMS Microbiol. Rev.* **32**, 149–167.
Vonrhein, C., Blanc, E., Roversi, P. & Bricogne, G. (2007). *Methods Mol. Biol.* **364**, 215–230.